Adaptive multichannel combining and equalization for underwater acoustic communications

M. Stojanovic, J. Catipovic,[a] and J. G. Proakis
Department of Electrical and Computer Engineering, Northeastern University, Boston, Massachusetts 02115

(Received 16 December 1992; accepted for publication 17 May 1993)

A theoretically optimal multichannel receiver for intersymbol interference communication channels is derived, and its suboptimal versions with linear and decision feedback equalizer are presented. A practical receiver based on any of these structures encounters difficulties in the underwater acoustic channels in which the extended time-varying multipath is accompanied by phase instabilities. A receiver that overcomes these problems by jointly performing adaptive mean-squared error diversity combining, multichannel carrier-phase synchronization and decision feedback equalization is proposed. Its performance is demonstrated on the experimental telemetry data from deep and shallow water long-range acoustic channels. Presented results indicate superior quality of coherent phase-shift keying (PSK) and quadrature amplitude modulation (QAM) reception obtained through joint equalization of very few channels.

PACS numbers: 43.30.Re, 43.60.Gk

INTRODUCTION

In the recent years there has been a growing interest in the underwater acoustic (UWA) communications in various application areas such as telemetry, remote control, speech, or image transmission. Consequently, the bandwidth efficiency of candidate systems becomes an important issue in UWA communications. While most of the existing systems use noncoherent modulation techniques, such as frequency-shift keying (FSK), in order to avoid problems associated with phase instabilities encountered in the UWA channels, current research focuses on the use of coherent modulation techniques which offer bandwidth efficiency and improved performance.

A large class of UWA channels can be characterized as rapidly varying time dispersive channels.[1] Although many of the radio communication channels fit into the same description, not all of the communication strategies developed for these channels have yet been successfully applied to the ocean channel. High-speed coherent digital communications over UWA channels are made difficult by the combined effect of extended time-varying multipath propagation and Doppler fluctuations. Multipath propagation is of special concern in horizontal links, where it results in very long channel responses spanning up to several tens of symbol intervals. The resulting intersymbol interference (ISI) makes the channel equalization disproportionately difficult as compared to that of most radio channels where multipath spreads are not larger than two or three symbol intervals. Even without the extended ISI, as is the case in vertical UWA links, reliable coherent communication over UWA channels is still a challenging task.

Some of the most recent work in this area[2–4] focuses on the use of differentially coherent modulation techniques such as differential phase-shift keying (DPSK). While Refs. 2 and 3 use linear equalization methods, Refs. 4 and 5 resort to the use of direct sequence spread spectrum (DS-SS) techniques to resolve and combat the ISI. Purely coherent modulation schemes, such as phase-shift keying (PSK), offer additional power efficiency, but face the problem of extracting the carrier reference in the presence of strong multipath. A receiver which deals with this problem by simultaneously performing adaptive equalization and synchronization was presented in Ref. 6. The experimental results of its application to long-range deep and shallow water, and short-range shallow water channels have demonstrated the feasibility of achieving coherent communications over these channels.

Further improvement in performance with respect to noise, as well as robustness to fading can be achieved through the use of spatial diversity. Since the concept of joint equalization and synchronization has proved to be an efficient way of dealing with various UWA channels, it is extended here to a multichannel case. The principles of diversity combining and those of equalization are well understood in communication theory,[7] but often used separately due to the fact that in many of the application areas it is usually one or the other that is needed. On the other hand, both the structure of the UWA channel, and the relative simplicity of building a receiver array, call for both multichannel combining and equalization in this channel. This paper deals with the theoretical and practical aspects of jointly optimal multichannel combining and equalization in the UWA channels.

We begin in Sec. I by reviewing the background theory of optimal multichannel combining for ISI channels, based on maximum likelihood sequence estimation (MLSE) principles. Using the analogy with single-channel receivers, suboptimal structures with linear and decision feedback equalizers (DFE) are deduced from the optimal receiver, and their parameters are optimized under the minimum mean-squared error (MMSE) criterion. Practical difficulties in operating the multichannel equalizer which arise in

[a]Woods Hole Oceanographic Institution, Woods Hole, MA 02543.

 0001-4966/93/94(3)/1621/11/$6.00 © 1993 Acoustical Society of America

loaded 07 Sep 2010 to 141.154.209.135. Redistribution subject to ASA license or copyright; see http://asadl.org/journals/doc/ASALIB-home/info/tern

the presence of large time-varying Doppler shifts are discussed in Sec. II, and a receiver which jointly performs MMSE multichannel combining, carrier phase recovery and fractionally spaced decision feedback equalization is presented. The receiver uses an adaptive algorithm which is a combination of recursive least squares (RLS) method and a second-order multichannel digital phase locked loop (DPLL), and can be implemented in a fast, numerically stable version. The algorithm is tested and proved efficient on experimental telemetry data, and some of the results are shown in Sec. III. The experiments, conducted by the Woods Hole Oceanographic Institution (WHOI), were performed in both deep and shallow water long-range UWA channels. The results demonstrate the fact that superior performance of coherent reception in UWA channels can be obtained through joint diversity combining and equalization.

I. OPTIMAL MULTICHANNEL COMBINING AND DATA DETECTION IN ISI CHANNELS

In this section we address the problem of extracting the transmitted data sequence from the signal received over a number of propagation paths and observed across an array of sensors. Due to the widespread use of linear beamforming in the UWA signal processing, it may seem natural to first use the array to beamform to each of the multiple signal reflections, and subsequently coherently combine the ISI free signals. However, the ML detector yields a different solution. The optimal ML combiner is shown to contain elements of a classical beamformer. However, it makes use of multiple arrivals, rather than treating them as an unwanted interference. In such a way, it benefits from the implicit time diversity present in the multipath propagation, as well as from the explicit, spatial diversity.

Let us assume the most general channel model in which each of the array sensors observes the transmitted signal passed through a different channel with some noise added. The transmitted signal is a data sequence linearly modulated onto a carrier, and it is represented in its equivalent complex baseband form as

$$u(t)=\sum_n d(n)g(t-nT), \tag{1}$$

where $\{d(n)\}$ is the sequence of M-ary data symbols, $g(t)$ is the basic transmitter pulse, and T the signaling interval. The channel, as seen by one of the K sensors, is described by its impulse response $f_k(t)$, which includes any transmit filtering. Both the effects of time delay and phase deviations are included in this response, and for the moment we treat $f_k(t)$ as constant in some interval of time T_{obs} in which the received signals are given by

$$v_k(t)=\sum_n d(n)f_k(t-nT)+\nu_k(t),$$
$$t\in T_{\text{obs}},\quad k=1,\ldots,K. \tag{2}$$

The term $\nu_k(t)$ represents zero mean additive noise which is independent of the data. In other words, no multipath effects are treated as noise.

In a special case of plane wave propagation, each of the received signals contains a number of reflections shifted in time across the array as given by

$$f_k(t)=\sum_{p=1}^{P} g_p[t-(k-1)T_p]e^{-j(k-1)\varphi_p},\quad k=1,\ldots,K, \tag{3}$$

where $g_p(t)$ is the response of the pth propagation path, T_p is the uniform delay between the array elements experienced by the signal traveling on that path, and φ_p is its corresponding phase angle. In matrix notation, this is expressed as

$$\mathbf{f}(t)=\mathbf{\Phi}\mathbf{g}(t). \tag{4}$$

In a narrow-band case, the operator $\mathbf{\Phi}$ reduces to matrix multiplication by

$$\mathbf{\Phi}=\begin{bmatrix} 1 & \cdots & 1 \\ e^{-j\varphi_1} & \cdots & e^{-j\varphi_P} \\ \vdots & & \vdots \\ e^{-j(K-1)\varphi_1} & \cdots & e^{-j(K-1)\varphi_P} \end{bmatrix} \tag{5}$$

and all the vectors are defined as column vectors. The received signals are arranged in a vector

$$\mathbf{v}(t)=\sum_n d(n)\mathbf{f}(t-nT)+\boldsymbol{\nu}(t)=\bar{\mathbf{v}}(t)+\boldsymbol{\nu}(t). \tag{6}$$

Assuming that the noise is temporally white Gaussian with covariance

$$E\{\boldsymbol{\nu}(t)\boldsymbol{\nu}'(t)\}=\mathbf{R}_\nu \tag{7}$$

the log-likelihood function of the data sequence $\mathbf{d}=\{d(n)\}$ is given by

$$\Lambda(\mathbf{d})=-\int_{T_{\text{obs}}}[\mathbf{v}(t)-\bar{\mathbf{v}}(t)]'\mathbf{R}_\nu^{-1}[\mathbf{v}(t)-\bar{\mathbf{v}}(t)]dt, \tag{8}$$

where prime denotes conjugate transpose. Maximizing this function with respect to the data sequence is equivalent to maximizing

$$L(\mathbf{d})=2\,\text{Re}\sum_n d^*(n)\int_{T_{\text{obs}}}\mathbf{f}'(t-nT)\mathbf{R}_\nu^{-1}\mathbf{v}(t)dt$$
$$-\sum_n\sum_m d^*(n)d(m)\int_{T_{\text{obs}}}\mathbf{f}'(t-nT)$$
$$\times\mathbf{R}_\nu^{-1}\mathbf{f}(t-mT)dt. \tag{9}$$

In the last expression we recognize the term

$$y(n)=\int_{T_{\text{obs}}}\mathbf{f}'(t-nT)\mathbf{R}_\nu^{-1}\mathbf{v}(t)dt \tag{10}$$

as the sum of the matched-filter outputs sampled at time nT. We use the notation

nloaded 07 Sep 2010 to 141.154.209.135. Redistribution subject to ASA license or copyright; see http://asadl.org/journals/doc/ASALIB-home/info/term

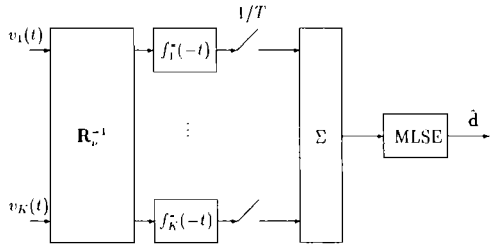

FIG. 1. Optimal multichannel receiver.

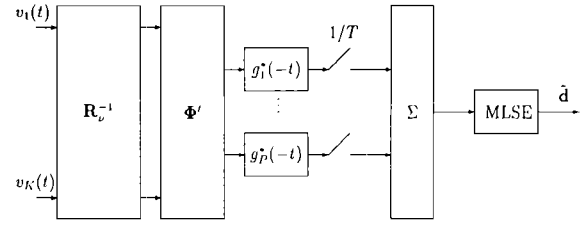

FIG. 2. Optimal narrow-band multichannel receiver.

$$R_{n,m}=R_{n-m}=\int_{T_{\text{obs}}}\mathbf{f}'(t-nT)\mathbf{R}_\nu^{-1}\mathbf{f}(t-mT)dt \quad (11)$$

and refer to this term as the composite channel autocorrelation function. With this notation the expression (9) is rewritten as

$$L(d)=2\,\text{Re}\sum_n d^*(n)y(n)-\sum_n\sum_m d^*(n)R_{n-m}d(m) \quad (12)$$

and the most likely transmitted data sequence is determined as

$$\tilde{\mathbf{d}}=\arg\max_{\mathbf{d}} L(\mathbf{d}). \quad (13)$$

The expressions (10) and (12) for the equivalent likelihood function suggest an optimal multichannel receiver structure as shown in Fig. 1. The optimal receiver consists of a combiner and a single-channel postprocessing algorithm for determining that data sequence $\tilde{\mathbf{d}}$ which has the largest likelihood given the combiner output and the knowledge of the composite channel autocorrelation function, subject to the constraint that data symbols take one of M possible values. The combiner itself consists of the $K\times K$ noise covariance inverse (in case of correlated Gaussian noise in each of the channels this would be a $K\times K$ linear filter), followed by a bank of matched filters each of which is matched to the channel as seen by the corresponding sensor. The matched-filter outputs are synchronously sampled using symbol rate sampling and coherently combined.

It may be interesting at this point to draw a parallel between the structure obtained and one that would employ a classical beamformer. For the sake of simplicity, let us concentrate on a narrow-band case, in which the propagation time between the array elements is much smaller than the symbol duration, $T_p \ll T$. In such a case, given the angles of signal arrivals from different paths, the optimal receiver has the structure as given in Fig. 2. It incorporates a $P\times K$ matrix transformation Φ' followed by a bank of filters matched to the individual path responses. In the simplest case, when there is no dispersion on individual paths, each of these filters is given by a complex channel gain multiplying the basic transmitter pulse. A classical beamformer on the other hand, designed to resolve the multiple arrivals based on their angular separation,[8] applies a matrix transformation $(\Phi'\Phi)^{-1}\Phi'$ on the input signals. It thus introduces additional noise correlation and results in the lower output SNR if followed immediately by matched filters. Therefore, we can say that the optimal beamforming, from the perspective of data sequence detection, is represented by the transformation Φ', whose task, together with that of matched filtering, is to weight signals from different channels and paths proportionally to their energy. In this manner, the optimal receiver coherently combines multiple reflections in each of the channels, making use of all of their energy, rather than using only one signal arrival per channel, as would have been the case with a classical beamformer. Similar arguments hold in a broadband case, except that the equivalent structure of the optimal receiver is somewhat more complicated.

Although theoretically identical, the two structures shown in Figs. 1 and 2 may lead to different implementations. In practice, the channel responses are not *a priori* known and are also time varying. Hence adaptive implementation is desirable, in which one can either make no assumptions about the spatial distribution of signals across the array, and implement the structure of Fig. 1, or one may resort to the angle of arrival estimation and implement a smaller, P-channel combiner of Fig. 2. The tradeoffs are many and largely depend on the ability to estimate and track the angles of arrival, provided that the plane-wave propagation assumption holds. Furthermore, in a practical implementation with finite length filters, there is a closed form MMSE solution for the first, but there is no closed form solution in the second case, due to the constrained structure of matrix Φ. We chose to concentrate on a K-channel combiner, since it requires no *a priori* knowledge of the channel structure, such as the number of multiple arrivals, which may be a difficult information to acquire for large range to depth ratios. It neither requires any particular array geometry, and can be used with as few as two sensors, which still provide diversity gain.

A. Optimal multichannel equalization

In many cases of practical interest, the computational complexity of the optimal structure becomes prohibitively high. For example, at a transmission range of three convergence zones in deep water, using a rate of 300 symbols per second, the ISI will span about 20 symbols, which makes even the Viterbi algorithm impractical to use. On the other hand, for shorter channel responses which result either at shorter ranges or at lower symbol rates, the use of the Viterbi algorithm aided by an adaptive channel estimator is a viable way of achieving high quality coherent communications. In order to reduce the computational com-

loaded 07 Sep 2010 to 141.154.209.135. Redistribution subject to ASA license or copyright; see http://asadl.org/journals/doc/ASALIB-home/info/tern

plexity, and make the multichannel receiver applicable to the long range UWA channels, we next consider suboptimal versions in which the MLSE block of the optimal receiver is replaced by a different detection algorithm. Essentially this is the problem of optimal multichannel combining and equalization. This problem was analyzed in Ref. 9 for linear and decision feedback equalizers, while we use here a simpler approach of merely deducing those structures from the optimal one, using sufficient statistics. Besides computational simplicity, the advantage of using an equalizer in place of the MLSE, is that it makes no assumptions about the underlying noise distribution.[10]

The expression (12) shows that the sequence $\{y(n)\}$ of combiner outputs represents the set of sufficient statistics for detecting the data sequence $\{d(n)\}$ since it is the only variable of the likelihood function that depends on the input signals. In other words, any multichannel equalizer structure, optimized under the MMSE criterion, will consist of exactly the same combiner part, while all the subsequent processing can be performed in a single channel, i.e., on the sequence $\{y(n)\}$ of combiner outputs. The problem of optimizing the multichannel equalizer parameters therefore reduces to the single-channel discrete time optimization problem. Using this fact, the classical principles of single-channel equalization techniques[7] can be directly applied to obtain the corresponding multichannel equalizers.

The combiner output, as a function of the desired data symbols, is given as

$$y(n)=\sum_k d(k)R_{n-k}+\xi(n), \tag{14}$$

where $\xi(n)$ is zero mean Gaussian noise with

$$E\{\xi(n)\xi^*(n-m)\}=R_m. \tag{15}$$

A linear symbol spaced equalizer with an infinite number of taps $\{a_n\}$ gives an estimate of the data symbol $d(n)$ as

$$\hat{d}(n)=\sum_k a_k y(n-k) \tag{16}$$

based on which final decision is made by quantizing it to the nearest symbol value. The MMSE solution for the equalizer transfer function is

$$A(z)=1/[1+R(z)], \tag{17}$$

where we have assumed that $E\{|d(n)|^2\}=1$, and

$$R(z)=\sum_m R_m z^{-m} \tag{18}$$

with R_m as given in Eq. (11).

The potential benefits of multichannel equalization are most easily seen in the case of spatially white noise. In this case $\mathbf{R}_v=\sigma_v^2\mathbf{I}$, and the composite channel spectrum $R(z)$ represents the sum of the individual channel's spectra, $R_k(z)$, normalized by the input noise power. Hence, if there is a spectral null in one of the channels $[R_k(e^{j\omega T})=0$ for some $\omega]$, in which case a single-channel equalizer would encounter difficulties, it does not imply a null in the composite spectrum $R(z)$, which is the one the multichannel equalizer is attempting to adjust to. At the same time,

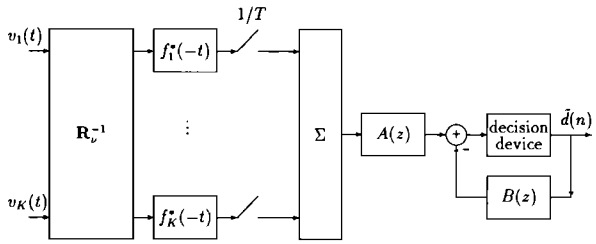

FIG. 3. Optimal multichannel DFE.

with more channels it becomes less likely that spectral nulls in different channels will coincide. In other words, the equalizer does not really see the individual channels, but only their coherent combination. Nevertheless, better performance is achievable if a decision feedback type of the equalizer is used.

The optimal multichannel DFE is obtained similarly using its single-channel counterpart. It consists of an optimal receiver's combiner part followed by a discrete time single-channel DFE, as shown in Fig. 3. The only function relevant for determining the DFE parameters is again the composite channel spectrum $R(z)$. The ideal DFE consists of an infinitely long anticausal feedforward filter $A(z)$ and the causal feedback filter $B(z)$. Using the spectral factorization[11]

$$R(z)+1=L(z)L^*(1/z^*), \tag{19}$$

where $L(z)$ denotes the causal and stable factor, the MMSE solution for the DFE filters is

$$A(z)=\frac{1}{L(0)L^*(1/z^*)}, \quad B(z)=\frac{1}{L(0)}L(z)-1. \tag{20}$$

In the stationary environment, both linear and decision feedback equalizers result in the steady state MSE equal to a_0, the zeroth tap of the corresponding feedforward filter. The DFE's MSE however is always smaller than that of the linear equalizer.

Our experimental results have indeed shown superior performance with a DFE, and the next section deals in detail with an adaptive implementation of a multichannel DFE. However, no matter which structure is used, similar problems concerning the adaptive implementation will arise, and the principles discussed in the next section are applicable to both the optimal and the structures with equalizers.

II. JOINTLY ADAPTIVE MULTICHANNEL CARRIER RECOVERY AND DECISION FEEDBACK EQUALIZATION

All the structures discussed so far were based on the assumption that the receiver has knowledge of the channel responses at all times. A practical receiver is aided by a channel estimator whose adaptation has to be carried out continuously to meet the rapidly changing conditions in the ocean channel. Knowledge of the channel responses involves knowledge of the multipath structure, propaga-

nloaded 07 Sep 2010 to 141.154.209.135. Redistribution subject to ASA license or copyright; see http://asadl.org/journals/doc/ASALIB-home/info/term

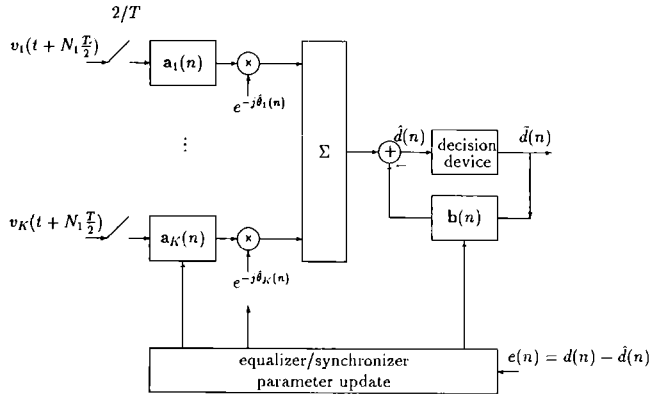

FIG. 4. Adaptive multichannel DFE.

tion delays and carrier phases. Of these three, carrier phase is by far the most rapidly changing parameter in the UWA channel. In classical communication systems, in which carrier and bit synchronization are performed separately from equalization, the presence of strong time-varying multipath affects the performance of a synchronization subsystem, resulting in poor tracking capabilities. The residual phase fluctuations on the other hand, impair the equalizer's performance, and may result in the tap rotation phenomenon.[12] The reason for this is that the rate of convergence of the equalizer tap update algorithm is lower than the rate at which the carrier phase changes. A possible solution to this problem is to jointly perform synchronization and equalization, and it appears to be particularly suitable for the UWA channels with severe multipath.[6]

The structure of an adaptive multichannel carrier phase synchronizer and DFE is shown in Fig. 4. The signals in all of the channels are frame synchronized prior to any processing. This is accomplished by matched-filtering to a known channel probe. The signaling frame is shown in Fig. 5. It consists of the channel probe, and a data block which itself starts with a training sequence. Frame synchronization is performed periodically, at the start of each frame, and it provides coarse alignment in time for the duration of a frame.

The overall channel response as a function of delay τ at time t can be written as

$$f_k(\tau,t)=h_k(\tau,t)e^{j\theta_k(t)}, \quad k=1,\ldots,K \tag{21}$$

so as to explicitly indicate the carrier phase $\theta_k(t)$ in each of the channels, and the more slowly varying part of the response $h_k(\tau,t)$. The received signal in the kth channel at time t is then given as

$$v_k(t)=\sum_n d(n)h_k(t-nT,t)e^{j\theta_k(t)}+v_k(t). \tag{22}$$

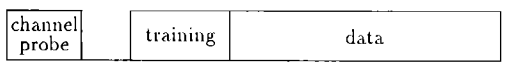

FIG. 5. Signaling frame.

These signals are sampled at a Nyquist or higher rate, and fed into the bank of feedforward fractionally spaced equalizers. Sampling is performed at an arbitrary initial time instant, and we assume a sampling rate of $2/T$ without loss of generality. This sampling rate is sufficient for signals bandlimited to $1/T$. The outputs of the feedforward filters are produced once per symbol interval, and since the fractionally spaced equalizers have the capabilities of analog filters[13] they implicitly account for symbol synchronization. Periodic frame synchronization ensures that the desired signal always stays within the time span of the equalizer, and no explicit symbol delay tracking is needed.

Looking at the structure of the receiver it is seen that there is no explicit linear equalization following the multichannel combiner as is the case in the optimal structure of Fig. 3. However, one can think of an alternative optimal structure in which the feedforward equalizer is moved into each of the matched-filtering branches. The functions of the feedforward section of the adaptive receiver now become apparent. It performs (1) adaptive matched filtering, (2) symbol synchronous sampling, and (3) linear equalization for reducing the ISI of future symbols. This temporal processing accounts for coherent combining of multiple arrivals in each of the diversity branches.

Following the feedforward filters is the multichannel carrier phase synchronizer. Depending on the particular channel characteristics, it may not be necessary to have a separate phase-locked loop (PLL) for each of the diversity branches if there is sufficient coherency between the carrier phases in different channels. In the application of interest, however, we found that due to the possibly large differences in time varying Doppler frequency offsets caused by unpredictable motion of the receiver array, it was necessary to have as many phase estimators as diversity channels. This is also one of the reasons that preclude the use of a passband DFE structure[14] in the multichannel form. In this structure, the carrier phase correction is moved further into the decision feedback loop, resulting in minor improvements.

After coherent combining, the signals from different channels are fed into the common decision feedback part of the equalizer. Since all the receiver parameters are updated jointly based on the single symbol estimation error, the performed spatial processing can be said to be of a maximal ratio combining type. In a pure maximal ratio (maximal SNR) combiner, which operates in conditions of no ISI, each diversity signal is weighted proportionally to its strength, and coherently combined with the others prior to decision making.[7] Indeed, if there were no ISI, the two structures would be equivalent. When there is ISI present, the multichannel receiver retains similar properties in the sense that if there is a channel with no signal in it, it will automatically be rejected in the process of adaptation, while the remaining channels will be favored according to their energy.

A. Receiver algorithm

Having established the receiver structure, we can proceed to determine the optimal values of its parameters. The optimization criterion we use is the minimum mean-

loaded 07 Sep 2010 to 141.154.209.135. Redistribution subject to ASA license or copyright; see http://asadl.org/journals/doc/ASALIB-home/info/tern

squared error between the estimated data symbol $\hat{d}(n)$ and the transmitted symbol $d(n)$. The receiver parameters to be determined are the tap weights of the multichannel feedforward equalizer, feedback equalizer coefficients, and the carrier phase estimates. In general, there are two ways of computing the equalizer parameters. One is the direct adaptation of the equalizer coefficients driven by the output error, and the other is their computation from the estimated channel impulse response. Although the latter is potentially more robust to the time variations of the channel,[16] we chose the usual, direct method, as computationally less involved.

Assuming the constant channel impulse response and carrier phase in some short interval of time, one arrives at the optimal values of equalization and synchronization parameters. Let the kth channel feedforward equalizer tap weight vector be

$$\mathbf{a}_k' = [a^k_{-N_1} \cdots a^k_{N_2}]^*, \tag{23}$$

where the tap weights are taken as conjugate for later convenience of notation. The input signal samples stored in the kth feedforward equalizer at time nT are represented in a vector

$$\mathbf{v}_k(n) = [v_k(nT + N_1T/2) \cdots v_k(nT - N_2T/2)]^T. \tag{24}$$

The output of the kth feedforward equalizer, after phase correction by the amount $\hat{\theta}_k$, is given as

$$p_k(n) = \mathbf{a}_k' \mathbf{v}_k(n) e^{-j\hat{\theta}_k} \tag{25}$$

and the coherent combination of all diversity channels is

$$p(n) = \sum_{i=k}^{K} p_k(n). \tag{26}$$

The feedback filter coefficients are arranged in a vector

$$\mathbf{b}' = [b_1 \cdots b_M]^* \tag{27}$$

and the vector of M previous decisions, currently stored in the feedback filter, is denoted as

$$\tilde{\mathbf{d}}(n) = [\tilde{d}(n-1) \cdots \tilde{d}(n-M)]^T. \tag{28}$$

This defines the output of the feedback filter as

$$q(n) = \mathbf{b}' \tilde{\mathbf{d}}(n). \tag{29}$$

The estimate of the data symbol at time n is

$$\hat{d}(n) = p(n) - q(n), \tag{30}$$

from which the decision $\tilde{d}(n)$ is obtained as the closest signal point. The estimation error is

$$e(n) = d(n) - \hat{d}(n) \tag{31}$$

and the receiver parameters are optimized based on joint minimization of the MSE with respect to $\{\mathbf{a}_k\}$, $\mathbf{b}$, and $\{\hat{\theta}_k\}$.

In order to find the optimal values of the equalizer coefficients, it is convenient to group all the coefficients into a composite vector $\mathbf{c}$, and to express the estimate $\hat{d}(n)$ as

$$\hat{d}(n) = [\mathbf{a}_1' \cdots \mathbf{a}_K' - \mathbf{b}'] \begin{bmatrix} \mathbf{v}_1(n) e^{-j\hat{\theta}_1} \\ \vdots \\ \mathbf{v}_K(n) e^{-j\hat{\theta}_K} \\ \tilde{\mathbf{d}}(n) \end{bmatrix} = \mathbf{c}' \mathbf{u}(n). \tag{32}$$

The MSE can now be expressed as a function of the composite equalizer vector $\mathbf{c}$, as

$$\begin{aligned} \text{MSE} &= E\{|d(n) - \mathbf{c}'\mathbf{u}(n)|^2\} \\ &= R_{dd} - 2\,\text{Re}\{\mathbf{c}'\mathbf{R}_{ud}\} + \mathbf{c}'\mathbf{R}_{uu}\mathbf{c}, \end{aligned} \tag{33}$$

where we have used the notation $\mathbf{R}_{xy} = E\{\mathbf{x}(n)\mathbf{y}'(n)\}$ for the cross correlations. The value of $\mathbf{c}$ that minimizes the MSE is the well known solution to the finite order Wiener filtering problem, and is given by

$$c = \mathbf{R}_{uu}^{-1} \mathbf{R}_{ud}. \tag{34}$$

The optimal values of the estimates of the carrier phases, $\hat{\theta}_k$, are most easily found if the estimate $\hat{d}(n)$ is represented as

$$\begin{aligned} \hat{d}(n) &= p_k(n) + \sum_{j \neq k} p_j(n) - q(n) \\ &= \mathbf{a}_k' \mathbf{v}_k(n) e^{-j\hat{\theta}_k} + \pi_k(n). \end{aligned} \tag{35}$$

The second term in the last expression is independent of $\hat{\theta}_k$, which makes it possible to express the MSE as

$$\begin{aligned} \text{MSE} &= E\{|d(n) - \pi_k(n) - \mathbf{a}_k' \mathbf{v}_k(n) e^{-j\hat{\theta}_k}|^2\} \\ &= -2\,\text{Re}\{\mathbf{a}_k' E\{\mathbf{v}_k(n)[d(n) - \pi_k(n)]^*\} e^{-j\hat{\theta}_k}\} \\ &\quad + \text{terms independent of } \hat{\theta}_k. \end{aligned} \tag{36}$$

The optimal values $\hat{\theta}_k$ satisfy the gradient equations

$$\begin{aligned} \frac{\partial \text{MSE}}{\partial \hat{\theta}_k} &= -2\,\text{Im}\{\mathbf{a}_k' E\{\mathbf{v}_k(n)[d(n) - \pi_k(n)]^*\} e^{-j\hat{\theta}_k}\} \\ &= 0, \quad k = 1, \ldots, K. \end{aligned} \tag{37}$$

In order to be able to track the time-varying optimal solution for the receiver parameters, the Eqs. (34) and (37) should be solved recursively, using updated values of possibly time-varying cross correlations. An alternative method to continuous adaptation is the so-called block adaptation,[17] in which the receiver parameters are updated only during short training blocks interspersed in the data stream, and interpolated between such blocks. The advantage of such an approach is the local prevention of error propagation.

As it was pointed out earlier, the carrier recovery process can theoretically be absorbed in the process of equalization. It can be verified that the optimal solution in such case would be the same as the one represented by Eqs. (34) and (37). The point of having separate expressions for the equalizer coefficients and the carrier phases, is to be able to derive different tracking strategies for the two, which ultimately eliminates the problem of equalizer tap rotation.

The simplest form of an adaptive algorithm is the combination of a least-mean-squares (LMS) algorithm for the equalizer coefficients update, and the first-order DPLL.[12]

nloaded 07 Sep 2010 to 141.154.209.135. Redistribution subject to ASA license or copyright; see http://asadl.org/journals/doc/ASALIB-home/info/term

Such an algorithm, however, failed on the UWA channel, primarily due to the poor phase tracking capabilities. In order to obtain improved phase-tracking capabilities, we introduce a second-order multichannel DPLL into the process of joint synchronization and equalization. Using the analogy between the phase detector output of a classical DPLL[15] and the instantaneous estimate of the MSE gradient with respect to $\hat{\theta}_k$, we define

$$\Phi_k(n)=\mathrm{Im}\{\mathbf{a}_k'\mathbf{v}_k(n)[d(n)-\pi_k(n)]^* e^{-j\hat{\theta}_k}\} \tag{38}$$

as the equivalent output of the kth phase detector. Using the fact that

$$d(n)-\pi_k(n)=p_k(n)+e(n) \tag{39}$$

the expression (38) is rewritten as

$$\Phi_k(n)=\mathrm{Im}\{p_k(n)[p_k(n)+e(n)]^*\}, \quad k=1,\ldots,K. \tag{40}$$

The second-order phase update equations are given by

$$\hat{\theta}_k(n+1)=\hat{\theta}_k(n)+K_{\theta_1}\Phi_k(n)+K_{\theta_2}\sum_{m=0}^{n}\Phi_k(m), \quad k=1,\ldots,K. \tag{41}$$

It is assumed here that the same proportional and integral tracking constants are used in all diversity channels, and that perfect loop integration is used. Alternative tracking strategies are of course possible.

The equalizer coefficients are computed adaptively based on the RLS estimation principles. The RLS algorithms have become almost a standard in digital signal processing, due to their superior convergence properties over the LMS algorithm. The RLS algorithm solves for the equalizer tap weight vector as

$$\mathbf{c}(n)=\hat{\mathbf{R}}_{uu}^{-1}(n)\hat{\mathbf{R}}_{ud}(n), \tag{42}$$

where the estimated cross-correlation matrices are $\hat{\mathbf{R}}_{xy}(n)=\Sigma_{m=0}^{n}\lambda^{n-m}\mathbf{x}(m)\mathbf{y}'(m)$, λ being the forgetting factor which accounts for the exponential windowing of the past data.[18]

The long channel responses which require long equalizers, in conjunction with diversity reception, result in high computational complexity if the standard RLS algorithm is used. Instead, a fast transversal filter (FTF) realization can be used for implementation. We have found a numerically stable FTF algorithm presented in Ref. 19 readily applicable for the problem at hand, with minor modifications concerning the incorporation of the carrier phases update equations. The computational complexity of the original algorithm is of the order of $10N$, and it can further be reduced by performing periodic instead of continuous update. With currently available processing speeds, and relatively low candidate symbol rates for the long-range UWA telemetry, the computational complexity is not a limiting factor. With 50 Mflops, and both feedforward and feedback equalizers of length 100, which is representative of the worst observed case for 1000 symbols per second transmission, up to 50 channels can theoretically be accommodated.

The exact performance analysis of the proposed receiver performance in a nonstationary environment is difficult to evaluate. The theoretical analysis of a similar receiver was carried out in Ref. 20 for the case of perfectly known and Rayleigh fading channel responses. The performance bounds for the optimal, infinite length multichannel DFE can be found in Ref. 9, again for perfectly known channels. It is the subject of current study to evaluate analytically the impact of estimation errors on the overall receiver performance, and the results obtained so far indicate possibly large losses at high fading rates. However, by increasing the signaling rate, the channel will stay relatively constant over a larger number of symbol intervals, at the expense of introducing the ISI. Since the proposed receiver is capable of compensating both for the ISI and phase fluctuations, it is suitable for use at high symbol rates, at which the long-range UWA channel stays relatively constant over a period of several hundreds of symbol intervals. This corresponds to moderate fading rates at which we expect no significant losses due to the channel mismatch.

III. EXPERIMENTAL RESULTS

The proposed algorithm was demonstrated on experimental telemetry data, and some of the results are presented here. The experiments were performed in two different long-range UWA channels, namely deep and shallow water channels. The fundamental difference between these two channels lies in the mechanism of sound propagation in each of them. In deep water, propagation occurs in convergence zones, while in the shallow water sound travels over a direct, and a number of bottom and surface reflected paths. Both channels are characterized by extended multipath, with coherence times on the order of a few seconds. The multipath spread was measured to be about 50 ms at 110 nautical miles in deep water, and about 100 ms at 50 nautical miles in the shallow water channel. Propagation in deep water results in a strong, but finite multipath, while the more random nature of reflections in the shallow water channel results in a typical channel response consisting of a fairly stable main arrival followed by an extremely long, unstable multipath. While both channels are typically nonminimum phase, the deep water channel has comparatively much more energy concentrated in the part of the response preceeding the main arrival. Both channels exhibit rapid and irregular phase fluctuations.

The deep water experiment was performed off the coast of northern California in January 1991. The transmission ranges were 40–140 nautical miles, corresponding to 1, 2, 3, and 4 convergence zones. The receiver had a vertical array of 12 sensors spanning depths from 500–1500 m. The shallow water experiment was performed at the New England Continental Shelf, in May 1992. In this experiment, the transmission ranges were 15–65 nautical miles, and the receiver was positioned in about 50-m-deep water with a vertical array of 20 sensors spanning depths

nloaded 07 Sep 2010 to 141.154.209.135. Redistribution subject to ASA license or copyright; see http://asadl.org/journals/doc/ASALIB-home/info/term

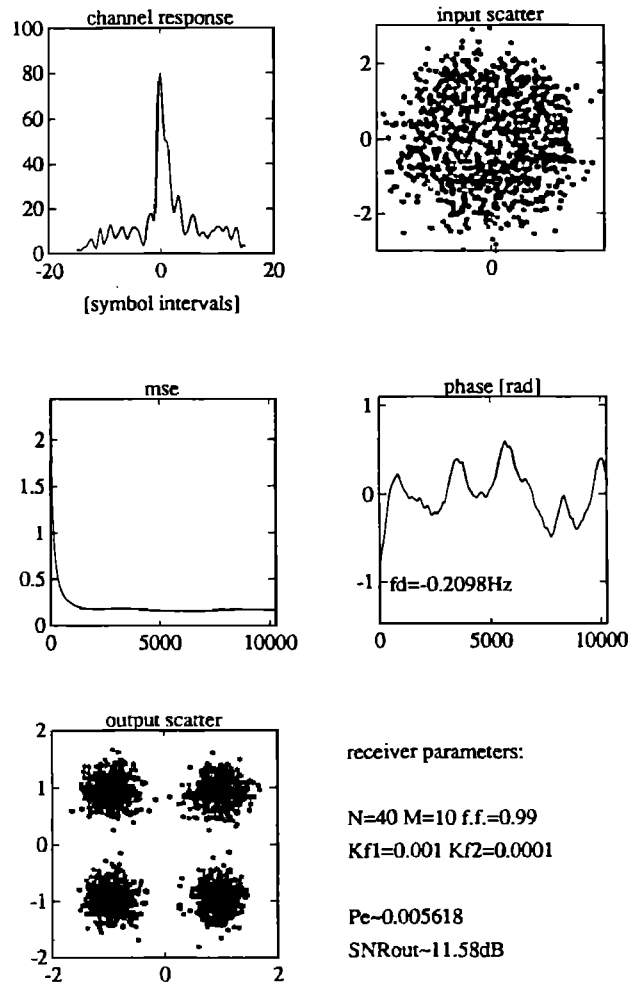

FIG. 6. Single-channel performance.

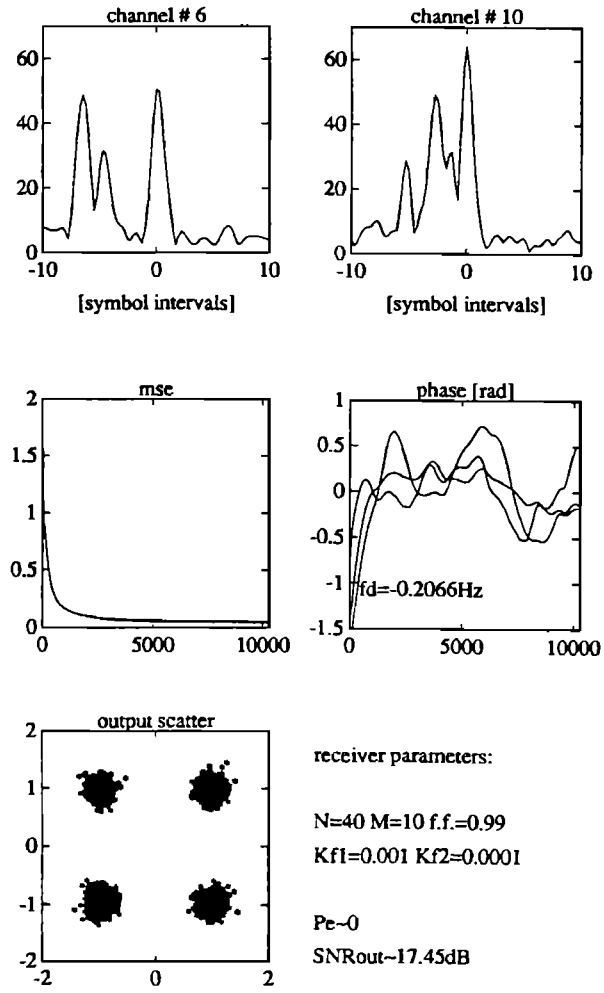

FIG. 7. $K=3$ multichannel performance.

from 15–35 m. The transmitter power in both experiments was 193 dB *re*: μPa, and a carrier frequency of 1 kHz was used.

The signaling frame, as shown in Fig. 5, was used with the channel probe consisting of a 13-element Barker code of symbols unshaped at the transmitter. The signals from the data blocks were shaped using a cosine roll-off filter with roll-off factor 0.5 and truncation length of ± 2 symbol intervals. The modulation formats were QPSK, 8-QAM, and 8-PSK, and the symbol rates were varied from 1–1000 symbols per second. The details of signal design are given in Ref. 21.

For purposes of later comparison, Fig. 6 shows an example of single-channel receiver performance in deep water at 110 nautical miles and 333 symbols per second signaling rate using QPSK modulation. The first subplot shows a snapshot of the channel response as obtained from the Barker probe and indicates the estimated input SNR of about 16 dB. Shown next to it is the input scatter plot which is completely smeared mostly due to the large amount of ISI present at this signaling rate. The algorithm converges in about 2–3 times the total number of taps used, and the mean-squared error plot shows this initial convergence and the proper operation in the subsequent, decision-directed mode. The estimate of the carrier phase, given in radians as a function of time measured in symbol intervals, indicates rapid and irregular variations. The scatter plot of the estimated data symbols $\hat{d}(n)$ shows the open eye, and

wnloaded 07 Sep 2010 to 141.154.209.135. Redistribution subject to ASA license or copyright; see http://asadl.org/journals/doc/ASALIB-home/info/terms

Range : 110 nautical miles

Rate : 333 symbols per second; 8-QAM

Channel # 8,10

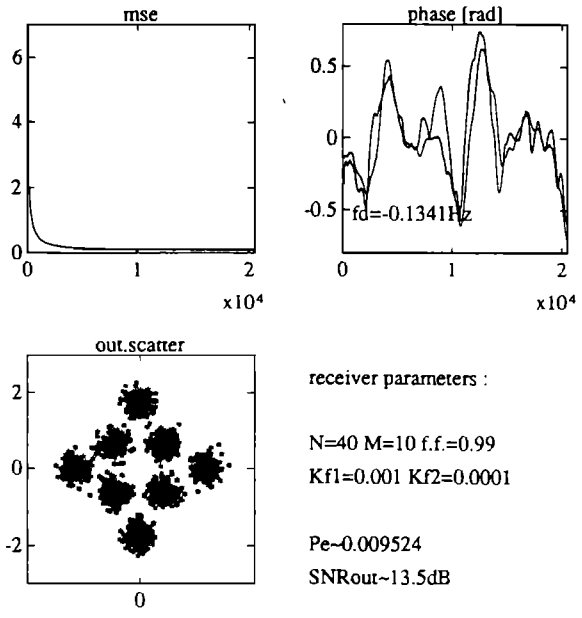

FIG. 8. $K=2$ multichannel performance.

the estimated probability of symbol error is on the order of 10^{-3}. The output SNR is defined as

$$\mathrm{SNR}_{\mathrm{out}}=10\log\frac{E\{|d(n)|^2\}}{(1/N_d)\Sigma_1^{N_d}|d(n)-\hat{d}(n)|^2}, \qquad (43)$$

with N_d the number of data symbols in a block, which is taken to be 10 000 for all the presented examples. In this case, $N=40$ feedforward, and $M=10$ feedback taps were needed, and these values, together with the forgetting factor of the RLS algorithm and the phase tracking constants are indicated in the figure.

Figure 7 shows the multichannel receiver performance obtained at the same range and rate with $K=3$ channels. The same channel as that of Fig. 6 was used together with two other channels whose instantaneous impulse responses are shown in Fig. 7. The channels are numbered according to depth, 0 being the one closest to the surface. The estimated phases are shown after the individual Doppler shifts of -0.18, -0.21, and -0.22 Hz were removed. The output eye pattern shows improvement of about 5 dB with respect to the single-channel output SNR. In this case, no errors were detected in a data block of length 10 000.

An interesting example shown in Fig. 8 is that of 8-QAM transmission over 110 nautical miles at 333 symbols per second. In this case, the single channel algorithm was not able to achieve a high enough output SNR needed

Range: 48 nautical miles

Rate: 500 symbols per second; 8-PSK

Channel # 2,4,6

SNRin~21 dB

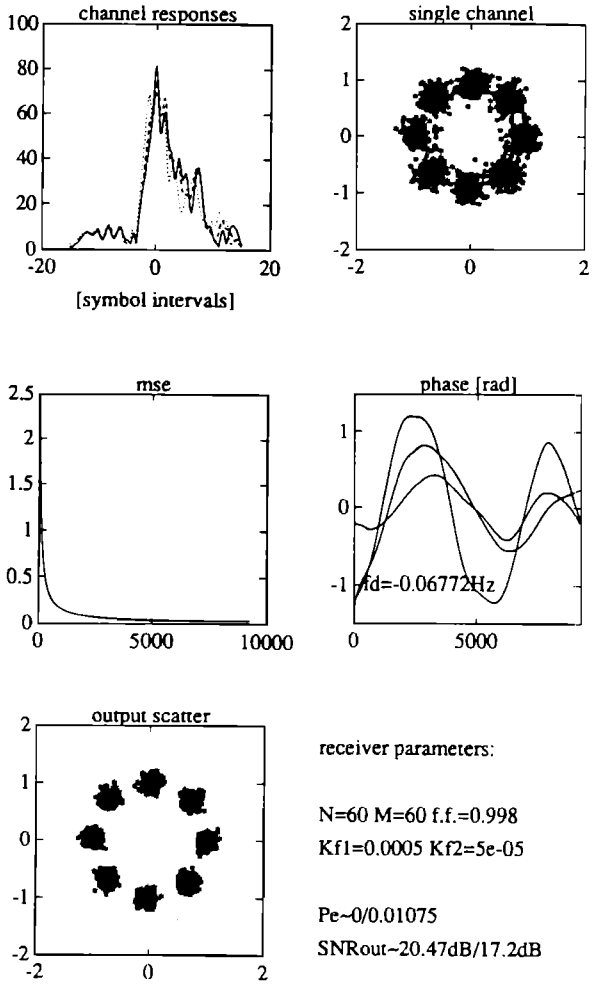

FIG. 9. Single- and $K=3$ multichannel performance.

for convergence in the decision-directed mode. However, by using only two channels in a multichannel algorithm, a relatively satisfactory performance was obtained as shown by the output scatter plot.

The shallow water performance results are shown in Fig. 9 for transmission over 48 nautical miles using a rate of 500 symbols per second. An 8-PSK modulation is used here which results in 1500 bits per second equivalent bit rate. Three channels are combined in this example, and the snapshots of their responses are shown in a single plot. There is much more coherence between the channels in this case due to the lower separation between the array elements. The input scatter plot in this case is again completely smeared, and rather than that one, we show the

loaded 07 Sep 2010 to 141.154.209.135. Redistribution subject to ASA license or copyright; see http://asadl.org/journals/doc/ASALIB-home/info/tern

output scatter plot resulting from the application of the single-channel algorithm. Although the single-channel algorithm converges, the related probability of symbol error is estimated to be on the order of 10^{-2}. Combining the three channels eliminates all the errors and results in about 3-dB better output SNR. It should be noted here that one cannot expect the gain of a pure, no ISI diversity combiner. The deviation from ideal is caused both by the presence of ISI and the noise enhancement in the feedforward equalizers. The amount of degradation depends on the channel structure and the length of the equalizers used. For example, in the case of 333 symbols per second QPSK transmission in deep water we obtained a 5-dB improvement by combining the same number of channels. Taking a closer look at the responses of these channels reveals the presence of a strong second arrival in one of the deep water channels. As it was discussed earlier, since the receiver is capable of synchronously processing multiple arrivals, such a channel structure brings an equivalent of time diversity gain. This fact, together with the fact that shorter equalizers were used in the deep water channel, explains the higher gain obtained in that case.

Finally, we examine the case of QPSK transmission at 1000 symbols per second over 48 nautical miles in shallow water, shown in Fig. 10. The channel in this case spans several tens of symbol intervals, requiring about 100 taps in the feedforward, and at least 80 taps in the feedback equalizer. The single channel performance in this case is limited by poor input SNR and extremely long multipath. Not to be forgotten is the fact that the carrier frequency is the same as the symbol rate used, and that the transducer bandwidth (700–1400 Hz) is actually smaller than that occupied by the signal. Nevertheless, the multichannel algorithm was able to achieve the error free performance in a block of 10 000 data symbols, resulting in noticeably clearer output eye pattern.

The results shown here correspond to the maximal rate/range combinations for which we were able to achieve good performance. Excellent results were obtained at all lower rates and ranges, while performance limitations were met at higher symbol rates and longer distances at which the available SNR was insufficiently high.

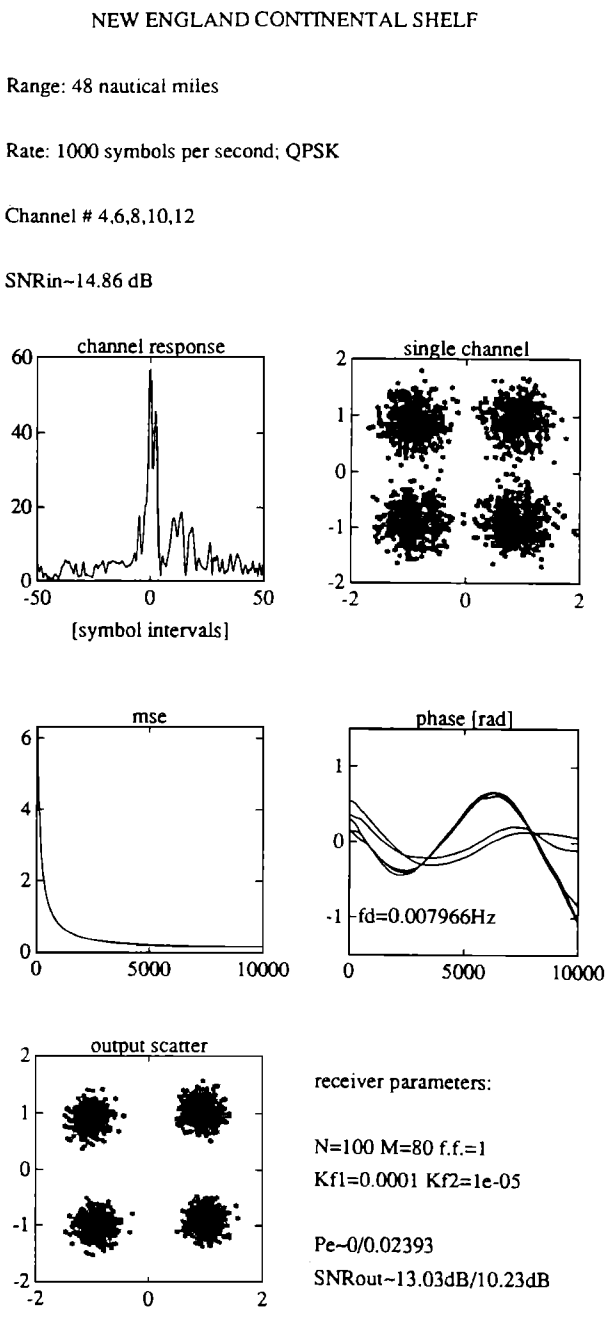

FIG. 10. Single- and $K=5$ multichannel performance.

IV. CONCLUSIONS

In order to improve the performance of a previously designed single-channel receiver for coherent demodulation of acoustically transmitted underwater communication signals, we considered its extension to the multichannel, spatial diversity case. The receiver structure that we used is based on the optimal multichannel DFE, but it incorporates a second-order multichannel DPLL which makes it possible to operate in the conditions of severe Doppler fluctuations met in the UWA channels. An RLS-based algorithm provides fast tracking capabilities needed for the highly dynamic ocean channel.

The receiver performs near-optimal spatial and temporal processing of the received signals by jointly performing MMSE multichannel combining and equalization. This results in both implicit diversity improvement obtained by coherent processing of multiple signal arrivals in each of the diversity channels, and the explicit diversity improvement obtained by coherent combining of signals from different channels.

Experimental results justify the earlier speculation that the approach of joint diversity combining and equalization is especially suited for achieving reliable high-speed digital communications over UWA channels. Long-range channels are representative of highly dispersive transmission medium and in addition they exhibit rapid Doppler fluctuations. With QPSK, 8-QAM, and 8-PSK signaling, satisfactory results were obtained with rates up to 300 symbols per second over three convergence zones in the deep water, and up to 1000 symbols per second over 50 nautical

nloaded 07 Sep 2010 to 141.154.209.135. Redistribution subject to ASA license or copyright; see http://asadl.org/journals/doc/ASALIB-home/info/term

miles in shallow water. The receiver algorithm is fully exploited on these channels, and is therefore certainly suitable for use in other, more benign UWA channels.

[1] J. Catipovic, "Performance limitations in underwater acoustic telemetry," IEEE J. Ocean. Eng. **OE-15**, 205–216 (1990).

[2] O. Hinton, G. Howe, and A. Adams, "An adaptive, high bit rate, sub-sea communications system," *Proceedings of the European Conference on Underwater Acoustics*, Brussels, Belgium, edited by M. Weydert (Elsevier Applied Science, Amsterdam, 1992), pp. 75–79.

[3] M. Suzuki and T. Sasaki, "Digital acoustic image transmission system for deep sea research submersible," in Proc. Oceans '92, Newport, RI (IEEE, New York, 1992), pp. 567–570.

[4] J. Fischer, K. Bennet, S. Reible, J. Cafarella, and I. Yao, "A high rate, underwater acoustic data communications transceiver," in Ref. 3, pp. 571–576.

[5] G. Sandsmark, A. Torsvik, and J. Hovem, "Shallow water coherent acoustic data transmission", in Ref. 2, pp. 88–91.

[6] M. Stojanovic, J. Catipovic, and J. Proakis, "Coherent communications over long range acoustic telemetry channels," *NATO ASI Series on Acoustic Signal Processing for Ocean Exploration*, edited by J. Moura and I. Lourtie (Kluwer Academic, Dordrecht, 1993), pp. 607–612.

[7] J. Proakis, *Digital Communications* (McGraw-Hill, New York, 1989).

[8] R. Monzingo and T. Miller, *Introduction to Adaptive Arrays* (Wiley, New York, 1980).

[9] P. Balaban and J. Salz, "Optimum diversity combining and qualization in digital data transmission with applications to cellular mobile radio," IEEE Trans. Commun. **COM-40**, 885–895 (1992).

[10] J. Proakis, "Adaptive equalization techniques for acoustic telemetry channels," IEEE J. Oceanic Eng. **OE-16**, 21–32 (1991).

[11] P. Monsen, "Feedback equalization for fading dispersive channels," IEEE Trans. Inf. Theory **IT-17**, 56–64 (1971).

[12] D. Falconer, "Jointly adaptive equalization and carrier recovery in two dimensional digital communication systems," Bell Syst. Tech. J. **55**, 317–334 (1976).

[13] R. Gitlin and S. Weinstein, "Fractionally spaced equalization: an improved digital transversal equalizer," Bell Syst. Tech. J. **60**, 275–296 (1981).

[14] S. Prasad and S. Pathak, "Jointly adaptive decision feedback equalization and carrier recovery in digital communication systems," AEÜ **43**, 135–143 (1989).

[15] W. C. Lindsey and C. M. Chie, "A survey of digital phase-locked loops," IEEE Trans. Commun. **COM-69**, 410–431 (1981).

[16] S. Fechtal and H. Meyr, "An investigation of channel estimation and equalization techniques for moderately rapid fading HF channels," Proc. ICC '91, 25.2.1–25.2.5 (1991).

[17] N. Lo, D. Falconer, and A. Sheikh, "Adaptive equalization and diversity combining for a mobile radio channel," Proc. Globecom '90, 923–927 (1990).

[18] S. Haykin, *Adaptive Filter Theory* (Prentice-Hall, Englewood Cliffs, NJ, 1986).

[19] D. Slock and T. Kailath, "Numerically stable fast transversal filters for recursive least squares adaptive filtering," IEEE Trans. Signal Process. **SP-39**, 92–114 (1991).

[20] P. Monsen, "Theoretical and measured performance of a DFE Modem on a fading multipath channel," IEEE Trans. Commun. **COM-25**, 1144–1153 (1977).

[21] J. Catipovic, L. Freitag, and G. Sandsmark, "Multiple convergence zone acoustic telemetry feasibility test report," WHOI-91-38 Technical Report, Woods Hole, MA (1991).

loaded 07 Sep 2010 to 141.154.209.135. Redistribution subject to ASA license or copyright; see http://asadl.org/journals/doc/ASALIB-home/info/tern